1991 SCA Conference Paper Number 9112

USE OF A HIGH MAGNETIC FIELD TO VISUALIZE FLUIDS IN POROUS MEDIA BY MRI

by
Catherine Chardaire-Rivière
and
Jean-Claude Roussel

Institut Français du Pétrole
Rueil-Malmaison, France

ABSTRACT

Magnetic Resonance Imaging (MRI) is very useful in core analysis because it gives information about petrophysical parameters: porosity and fluid saturations. This paper deals with several applications of MRI to the study of fluid distribution in porous media, with a strong 9.4 tesla magnetic field. The use of a strong magnetic field coupled with high gradients produces images with good resolution and enables very thin slices to be obtained.

Oil and water were visualized in small core samples (1 cm in diameter and 2.5 cm in length). The MRI profiles were compared to those from a numerical simulator based on generalized Darcy's law. Good agreement was observed between experiment and simulation showing the validity of MRI profiles.

A 3-D reconstruction of oil distribution was presented for oil and gas. The 3-D visualization showed a preferential path for gas.

INTRODUCTION

Visualizing fluid distribution in a porous medium is very helpful in the study of multi-phase flow in porous media. Visualization may be done by gamma-ray attenuation technique (Bourbiaux et al. 1990). But in some cases -- for example fluid flow fingering -- a one-dimensional description is not sufficient and a two- or three-dimensional description is required. X-ray tomography is the first way to get a two-dimensional description of a rock sample so as to obtain 2-D images of porosity or visualize displacement in a porous medium (Withjack et al. 1990). Fluid distribution images result from substracting the image of the rock matrix from fluid-saturated rock images. MRI is the second way to obtain 2-D images. Unlike X-ray tomography, which visualizes both the rock matrix and fluids, MRI visualizes only fluids and the interaction of these fluids with the surface of the pores.

MRI is an extension of Nuclear Magnetic Resonance (NMR), a technique explained in Ernst et al. 1987. The nucleus of some atoms has nuclear moment which may interact with a magnetic field. When such atoms are placed in a magnetic field and excited with a radiofrequency pulse a transient signal follows which is detected in a coil placed around the sample. The amplitude and frequency of the signal depend on the strength of the magnetic field and are characteristic of both the nucleus and of its chemical environment. Spatial discrimination is required to get an image of the distribution of a kind of nucleus. Discrimination is produced by superposing three orthogonal linear magnetic field gradients on the main magnetic field. In this way each point of the sample is subjected to a different magnetic field, and so gives a signal at a different frequency which is related to a spatial position. If only one gradient in one direction is used a discrimination of the signals only in this direction is obtained. This is how an amplitude profile is got. In a strong magnetic field it is also possible to differentiate between species having the same nucleus and study them in a different environment. An example is studying protons and obtaining an image of oil and of water in core samples containing oil and water. The chemical shift method is used to do this.

Various nuclei can be studied by NMR, but only proton, deuteron and carbon 13 are relevant for petrophysical applications (see Chardaire and Roussel, 1990). The use of NMR for petrophysical applications was first extended to MRI in 1979, when Gummerson et al. used NMR to monitor capillary absorption of water in a plaster bar. They obtained one-dimensional profiles indicating the quantity of water absorbed as a function of time. The first image was published in 1985 by Rothwell and Vinegar and showed Berea sandstone containing water. Since then, many papers have been published describing the use of MRI to visualize fluids. Chemical shift methods were used to visualize water or oil selectively (Hall et al. 1987, Horsfield et al. 1989, Dechter et al. 1989), or one of the two phases was doped to cancel out its signal (Blackband et al. 1986, Chen et al. 1988, Baldwin et al. 1989, Guillot et al. 1989). Deuteron imaging was coupled with proton imaging to differentiate between oil and water (Mahmood et al. 1990). Images of flow were also obtained (Woessner et al. 1990).

In this investigation a strong magnetic field of 9.4 tesla enabled to have very thin slices. The apparatus and core samples used will first be described, then the coreflood tests studied by MRI and finally a 3-D reconstruction of oil distribution will be shown.

EXPERIMENTAL

Two cylindrical porous media were used for the different experiments: Fontainebleau sandstone (pure quartz) with a porosity of 22 % and a gas permeability of 1500 mD and bioclastic limestone with a porosity of 30 % and a gas permeability of 300 mD. The rock samples were 2.5 cm (0.98 in.) in length and 1.0 cm (0.39 in.) in diameter. They were laterally coated with an epoxy resin, so the external diameter of the coated samples was 2.0 cm. Both core samples were strongly water wet. MRI images were obtained at 9.4 tesla with a Bruker MSL-400 spectrometer which can be used in either a spectrometer or a micro-imaging configuration. Only hydrogen can be observed in the micro-imaging configuration, and 9.4 tesla corresponds to a frequency of 400 MHz for protons. Radio frequency coils were placed on removable inserts that could be adapted to the probe. Several inserts could have been used ranging from 0.25 to 2.5 cm (the first ones perpendicular to the magnetic field, the others parallel). The 2.5 cm insert was used in all the experiments to study samples 2.0 cm in diameter. The height of the coil was then 5.0 cm, but the sample itself was shorter (2.5-3.0 cm) to prevent image distortion at both ends.

Gradient coils were supported by the probe itself to facilitate the change from spectrometer to micro-imaging configurations. Their strength can reach 50 G/cm, but such high gradients involve great sweep width and consequently low digital resolution. Gradients from 7 to 15 G/cm were used. Slice gradient could be decreased to get a slice thickness with a sufficient signal. Slices 50 μm thick can be obtained with such gradients. Two kinds of pulse sequences were used: a standard spinwarp sequence to obtain an image of all the hydrogens in the sample, and a selective chemical shift sequence giving an image of water or oil alone. A hard 90° pulse of 42 microseconds (μs) was used in the spinwarp sequence. In the chemical shift sequence, it was a soft 90° pulse centered on the chemical shift of the species observed. Echo time was usually 8 milliseconds (ms) and could be reduced to 6 ms. It was possible to get images parallel or perpendicular to the magnetic field, and image size was 256 x 256 pixels. Within the image the resolution was about 100 μm. Ten-hour images were made to increase the signal over noise ratio, but satisfactory images could be made in about one hour.

The difference between oil and water chemical shifts is about 1500 Hz for a 9.4 tesla magnetic field. The two oil and water signals were well separated in the limestone sample, but not in the sandstone as signal widths were broader. The broad linewidths were mainly due to the difference between the static susceptibility of the rock matrix and the fluid (Glasel et al. 1974). The

difference is greater for sandstone than for limestone. So oil and water were used for the displacement experiment in the limestone sample and the chemical shift sequence gave an image for oil and for water. Oil and heavy water (D_2O) instead of water were used for the sandstone sample, and the spinwarp sequence visualized the oil signal. D_2O does not emit a NMR signal at the proton resonance frequency.

All the spectrometer results were transmitted by ETHERNET network onto a SUN associated with a PIXAR computer specialized in image treatment, and onto a VAX for the profile computing.

DISPLACEMENT EXPERIMENTS

Displacement experiments were performed on the two core samples previously described. Since imaging time was so long, it was important to prevent any fluid redistribution during acquisition time. Because the cores are strongly water wet, drainage tests (i.e. non wetting fluid saturation increasing) were studied. The oil was injected at the top of the sample to get a stabilizing effect of gravity. This was maintened during acquisition because the samples were vertical in the magnetic field. The flow was stopped between two injections so that the sample could be placed in the magnetic field.

About ten pore volumes of refined oil (Soltrol 130) were injected into the limestone sample saturated with water. No further change in saturation was expected after this lengthy injection. As previously explained, it was possible to use the chemical shift sequence in such a mineral to separate the oil signal from the water signal. Figure 1 shows oil distribution inside the rock in the direction of the flow, and Figure 2, water distribution. Here high gradients (14 G/cm) gave slices 50 μm thick. These results were already partially presented (Chardaire and Roussel 1990).

It was not possible to separate the oil signal from the water signal for the Fontainebleau sandstone. So we chose heavy water (D_2O) instead of water. The D_2O was of a minimum purity of 99.6 atom %D. Oil distribution inside the core was monitored by the spinwarp sequence. A water-oil drainage experiment was performed on the Fontainebleau sandstone. The core was initially 100 % saturated with deuterated water and the oil was injected from top to bottom at a constant pressure drop. Core petrophysical properties and experimental conditions are given in Table 1. As the core sample was very small, the pore volume was too low to measure fluid production accurately. The measurements during displacement consisted of profiles indicating oil distribution. Figure 3 gives the profiles before injection (no oil signal) and after three injection times: 10 sec, 40 sec, and 745 sec. After displacement, the core was cleaned and fully saturated with oil. This profile is also shown in Figure 3. Only the cumulative volume of fluid injected was evaluated in the profile. The MRI profiles were constructed with a measurement every 0.013 cm. 186 measurements were made for the 2.5 cm of the core. The profiles were obtained by using one magnetic field gradient parallel to the displacement. The signal was accumulated 32 times in each profile, and it took about 3 mn to get each one .

Mandava et al. 1990, explained how to calculate saturation profiles from MRI profiles. At a given position z along the profile, the amplitude I(z) in a spinwarp sequence is:

$$I(z) = F\, S(z)\, e^{-\frac{TE}{T_2}} \left(1 - e^{-\frac{TR}{T_1}}\right) \qquad (1)$$

where F depends on many factors such as receiver gain, static magnetic field and receiving coil quality factor.

T_1 and T_2 are the relaxation times of oil in the core sample, and TE and TR are characteristic NMR experiment times. S(z) is linear spin density which is proportional to oil saturation. So oil saturation profiles can be obtained by using the profile for the fully oil-saturated core sample measured under the same conditions (TE and TR equal). Figure 4 gives the three oil saturation profiles from MRI profiles.

Mandava et al. 1990, developed a criterion for image acquisition time Texp, to ensure that the accuracy of saturation determination is not limited by the dynamic nature of the experiment.

$$\frac{v\ Texp}{\emptyset \Delta z} \leq \varepsilon \qquad (2)$$

See the nomenclature for definitions.
As this displacement experiment was performed at constant pressure, it was not easy to calculate the superficial velocity, v.

Moreover, Mandava at al. also studied the accuracy with which saturations are determined. They found that accuracy would in no case exceed $\pm$ 0.05 saturation units. Different MRI profiles were obtained at different times with the fully oil-saturated sample for the displacement considered here. Their variation proved to be in this range.

A numerical simulator verified the validity of the MRI profiles by comparing experimental MRI profiles and simulated ones. The numerical simulator was described in previous papers (Chardaire et al., 1989, 1990). Its main characteristics are:

- Two-phase displacements in laboratory experiments are represented by a one-dimensional, two-phase incompressible model based on generalized Darcy's law. Experiments can be studied at a given flow rate or pressure drop.

- Various boundary conditions enable the simulation to be made for the following laboratory experiments: forced drainage, gravity drainage, forced imbibition and free imbibition.

- Relative permeabilities and capillary pressure can be determined. They are estimated by using a least-squares technique after the one-dimensional saturation equation has been solved. The experimental data required are: the outlet production, pressure drop between the two faces and, or local saturation profiles measured at different times in the sample.

Average petrophysical parameters were measured in the experiment, but relative permeability curves were not available. The capillary pressure curve was determined on a companion plug. So MRI saturation profiles were used to determine relative permeability and capillary pressure curves from numerical simulations. In the least-squares problem, the experimental capillary pressure curve was used as the first input data and straight lines initially as relative permeability curves.

The overall shape of experimental profiles was quite well reproduced by simulation. Excellent agreement was observed for the third saturation profile corresponding to the vicinity of residual water saturation. Agreement between the experiment and simulation was less good for the first and the second saturation profiles. The experimental profile for the core fully saturated with oil demonstrated that the core was not absolutely homogeneous (see Figure 3). Porosity was lower in the first part of the core than in the second. This probably also induced variation in local

permeability. Local heterogeneities were not taken into account in simulation since the core was considered homogeneous. This could explain the differences observed between experimental and simulated profiles. The MRI profiles are shown to be valid when the two sets of profiles are compared, however. The relative permeability and capillary pressure curves that were identified and then used in simulations are plotted on Figures 6 and 7 respectively. Identified capillary pressure is close to the experimental one.

MRI saturation profiles coupled with a numerical simulator give both relative permeability and capillary pressure curves representative of a displacement. The time necessary to get profiles is very short compared to displacement time. This method can be used to determine petrophysical characteristics on very small samples from side wall coring, for example. NMR technique can also be extrapolated to larger cores of course, provided adequate NMR equipment is available.

3-D IMAGING

Gas was injected into the sandstone sample fully saturated with oil, and injection was stopped when the gas breaktrough appeared. Then 13 slices were taken from the sample by using a multislice experiment. Here the gradient strength was 4.9 G/cm, each slice was 240 μm thick.

Slices were separated from one another by 0.14 cm. The ETHERNET network transferred the slices onto a SUN associated with a PIXAR computer. The PIXAR's main characteristics are : each pixel coded on 64 bits (16 bits for red, 16 for green, 16 for blue and the remaining 16 for transparency), specialized software for 3-D data volume reconstruction based on volume rendering techniques, that can generate high-quality images of 3-D geometric models in minutes.

As the MRI slices were not contiguous, each one was duplicated to reach a final volume with the same size as the real sample. Only oil distribution was seen in the images, gas did not emit a sufficient signal. The 13 slices are shown in Figure 8. Four views of the PIXAR reconstruction are given in Figure 9.

The 3-D image shows that oil distribution is not homogeneous for liquid displaced by gas. The gas flows along a preferential path. Here, numerical simulation based on a one-dimensional model does not represent displacement mechanisms accurately. 3-D representation is an indispensable tool in understanding such flows.

CONCLUSIONS

This paper deals with some results concerning visualization of fluids inside a porous medium during a flooding experiment at 9.4 tesla. The feasibility of using NMR with high magnetic fields has been demonstrated to visualize immiscible fluids inside porous media.
The results obtained on Fontainebleau sandstone and on a limestone show :

i) the possibility of obtaining an image of a slice 50 μm thick,

ii) the validity of the profiles obtained by MRI and the possibility of using MRI as a tool to determine both relative permeability and capillary pressure curves.

iii) the use of NMR as a tool to study displacement in three dimensions.

ACKNOWLEDGEMENTS

The authors wish to thank C. Lallemand who made the 3-D reconstruction, and D. Longeron for his comments concerning the coreflood tests.

NOMENCLATURE

F	constant of proportionality
TE	echo time
TR	repetition time
T1	longitudinal relaxation time
T2	transverse relaxation time
S(z)	linear spin density
v	superficial velocity
Δz	length of a pixel
Texp	acquisition time
ϕ	porosity
ε	error in saturation

REFERENCES

Baldwin B.A., Yamanashi W.S., 1989 : "Detecting Fluid Movement and Isolation in Reservoir Cores with Medical NMR Imaging Techniques". SPE Reser. Eng. May, 207-212.

Blackband S., Mansfield P., Barnes J.R., Clague A.D.H., Rice S.A., 1986 : "Discrimination of Crude Oil and Water in Sand and in Bore Cores with NMR Imaging". SPE Formation Evaluation. Feb. 31-34.

Bourbiaux B.J., Kalaydjian F.J., 1990 : "Experimental Study of Concurrent and Countercurrent Flow in Natural Porous Media". SPE Reservoir Engineering, August.

Chardaire C., Chavent G., Jaffre J., Liu J., Bourbiaux B., 1989 : "Simultaneous Estimation of Relative Permeabilities and Capillary Pressure". SPE 19680 presented at the 64th Annual Technical Conference and Exhibition of the SPE, San Antonio, Oct. 8-11.

Chardaire C., Roussel J.C., 1990 : "NMR Imaging of Fluid Saturation Distributions in Core Samples Using a High Magnetic Field". 1st European Core Analysis Symposium, London 21-23 May.

Chardaire-Rivière C., Chavent G., Jaffre J., Liu J., 1990 : "Multiscale Representation for Simultaneous Estimation of Relative Permeabilities and Capillary Pressure". SPE 20501 presented at the 65th Annual Technical Conference and Exhibition of the SPE, New-Orleans, Sept. 23-26.

Chen J.D., Dias M.M., Patz S., Schwartz L.M., 1988 : "Magnetic Resonance Imaging of Immiscible Fluid Displacement in Porous Media". Physical Review Letters. Vol. 61, Number 13, 26 sept.

Dechter J.J., Komoroski R.A. and Ramaprasad S., 1989 : "NMR Chemical Shift Selective Imaging of Individual Fluids in Sandstone and Dolomite Cores". SCA Conference paper number 8903, New Orleans.

Ernst R.R., Bodenhausen G., Wokaun A., 1987 : "Principles of Nuclear Magnetic Resonance in One and Two Dimensions". Oxford Science Publications, Oxford.

Glasel J.A., Lee K.H., 1974 : "On the Interpretation of Water Nuclear Magnetic Resonance Relaxation Times in Heterogeneous Systems". J. Amer. Chem. Soc. 96, 970.

Guillot G., Trokiner A., Darasse L., Saint-Jalmes H., 1989 : "Drying of a Porous Rock Monitored by NMR Imaging". J. Phys. D: Appl. Phys. 22 1646-1649.

Gummerson R.J., Hall C., Hoff W.D., 1979 : "Unsaturated Water Flow within Porous Materials Observed by NMR Imaging". Nature Vol. 281, 6 Sept.

Hall L.D., Rajanayagam V., 1987 : "Thin-Slice, Chemical-Shift Imaging of Oil and Water in Sandstone Rock at 80 Mhz". Journal of Magnetic Resonance 74. 139-146.

Horsfield M.A., Fordham E.J., Hall C., Hall L.D., 1989 : "^{1}H NMR Imaging Studies of Filtration in Colloidal Suspensions". Journ. of Magnetic Resonance 81. 593-596.

Mandava S.S., Watson A.T., Edwards C.M., 1990 : "NMR Imaging of Saturation During Immiscible Displacements". AICHE Journal, Vol. 36, N° 11, p. 1680-1686, November.

Mahmood S., Doughty D., Tomutsa L., Honarpour M.M., 1990 : "Pore Level Fluid Imaging Using High Resolution Nuclear Magnetic Resonance Imaging and Thin Slab Micromodels". SCA conference paper number 9024.

Rothwell W.P. and Vinegar H.J., 1985 : "Petrophysical Applications of NMR Imaging". Applied Optics 1 Dec., vol. 24, N° 23.

Withjack E.M., Graham S.K., Yang C.T., 1990 : "Determination of Heterogeneities and Miscible Displacement Characteristics in Corefloods by CT Scanning". SPE paper 20490, 65th Annual Technical Conference and Exhibition of the SPE, New-Orleans, Sept. 23-26.

Woessner D.E., Gleeson J.W., Jordan C.F., 1990 : "NMR Imaging of Pore Structures in Limestone". Paper SPE 20493 presented at the 65th Annual Technical Conference and Exhibition of the SPE, New Orleans, Sept. 23-26.

Table 1
Core Properties and Operating Conditions for Laboratory Drainage Experiment

Core length	2.5 cm
Area of core section	1.04 cm^2
Average Porosity	0.22
Permeability	1200 mD
Water density	1.1 $g.cm^{-3}$
Oil density	0.76 $g.cm^{-3}$
Water viscosity	1 mPa.s
Oil viscosity	1.3 mPa.s
Pressure drop	0.045 Bar
Initial water saturation	1
Residual water saturation	0.3

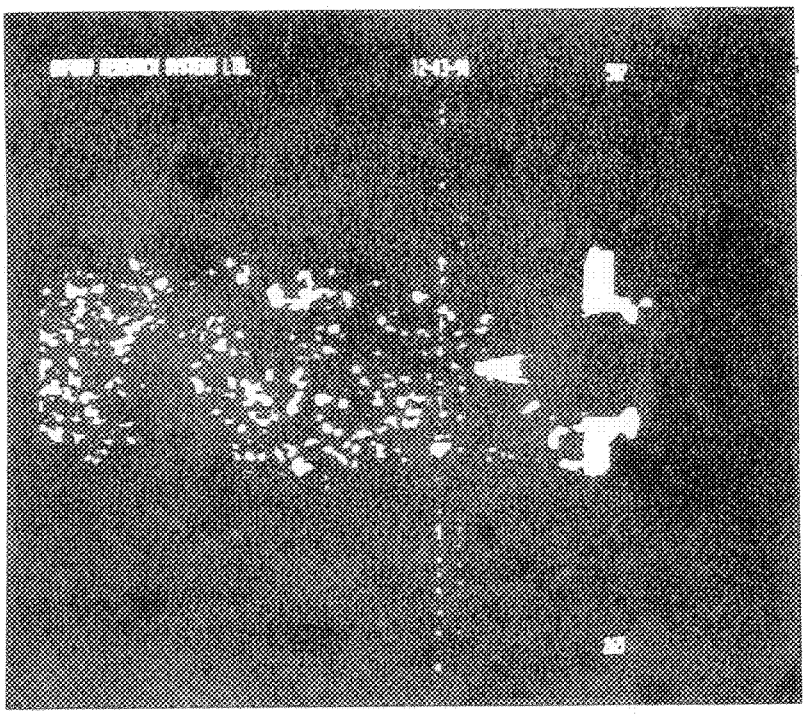

Figure 1 : Slice 50 μm thick showing oil distribution inside the porous medium containing oil and water.

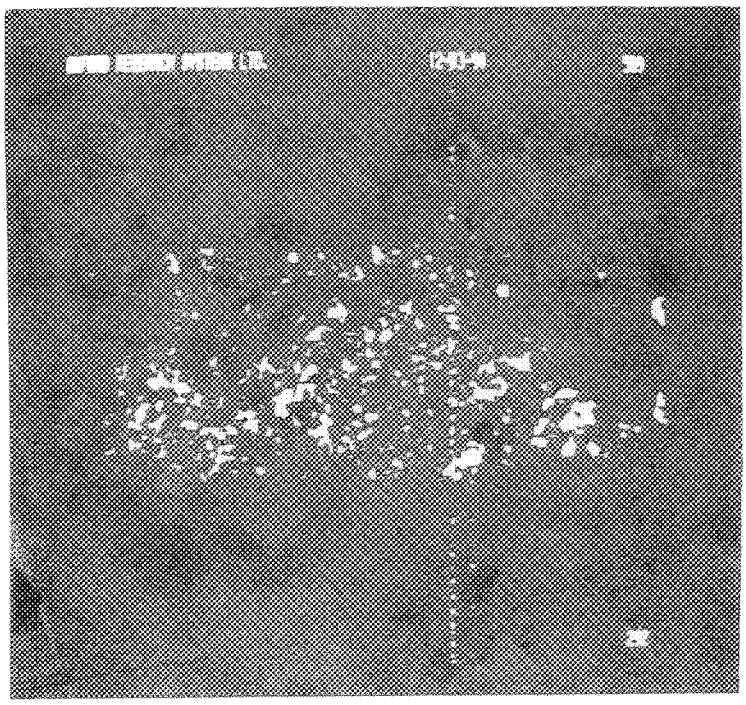

Figure 2 : Slice 50 μm thick showing water distribution inside the porous medium containing oil and water.

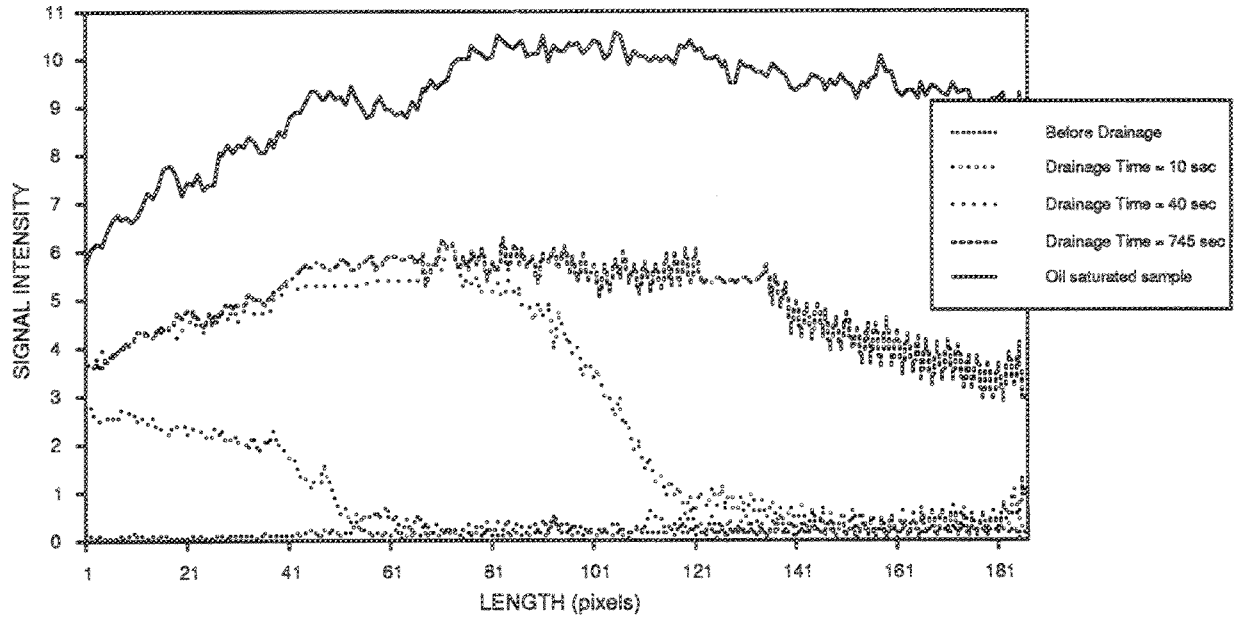

Figure 3 : Experimental profiles showing oil distribution.

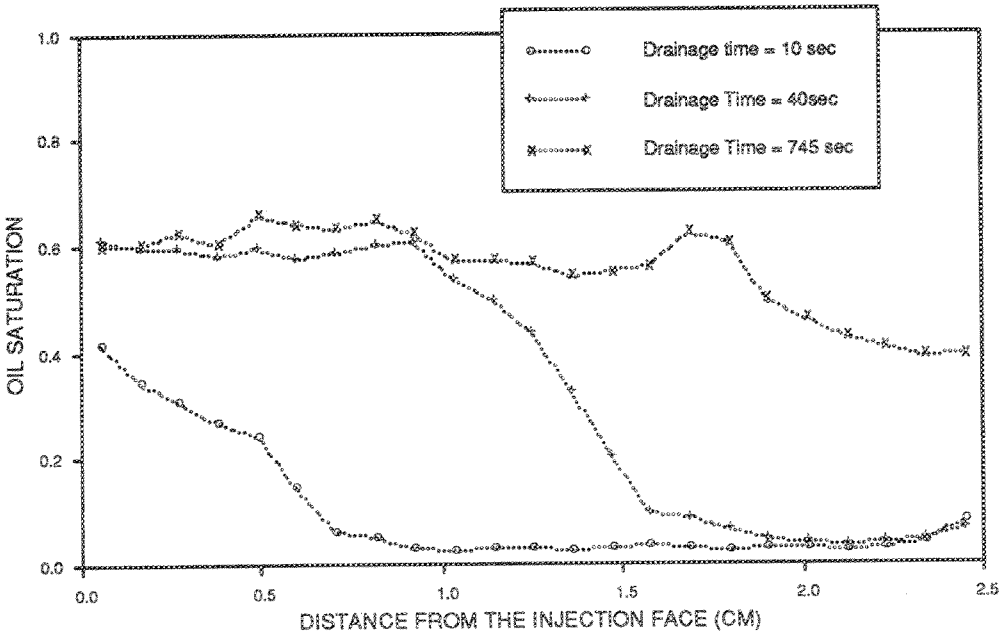

Figure 4 : Saturation profiles from MRI profiles.

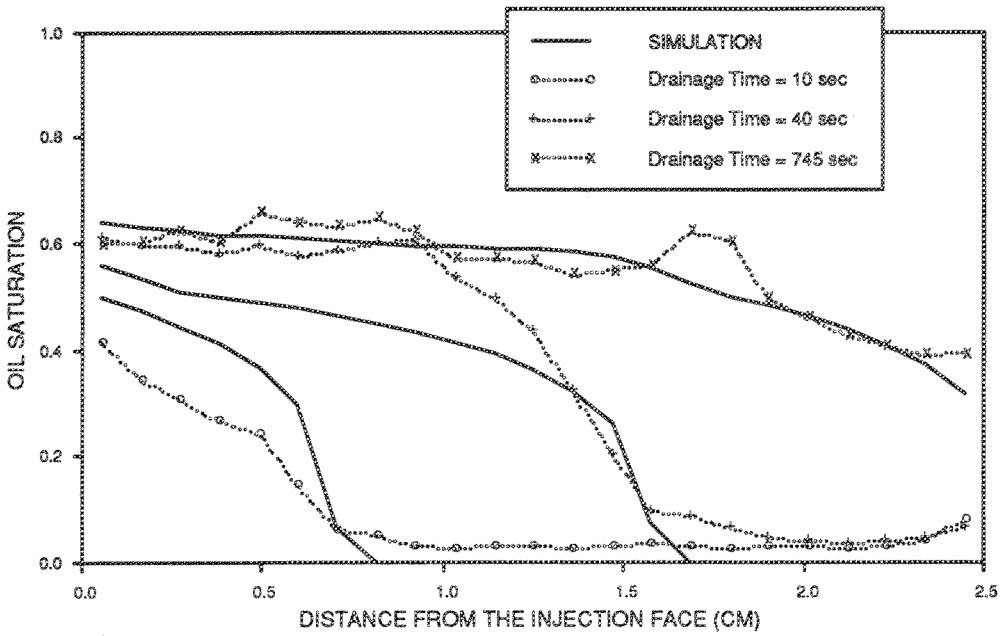

Figure 5 : Comparaison between experimental MRI profiles and simulated profiles.

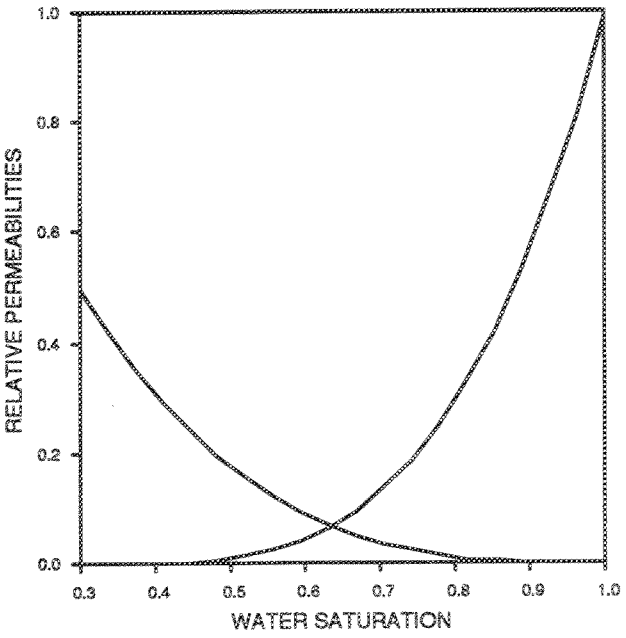

Figure 6 : Estimated relative permeability curves.

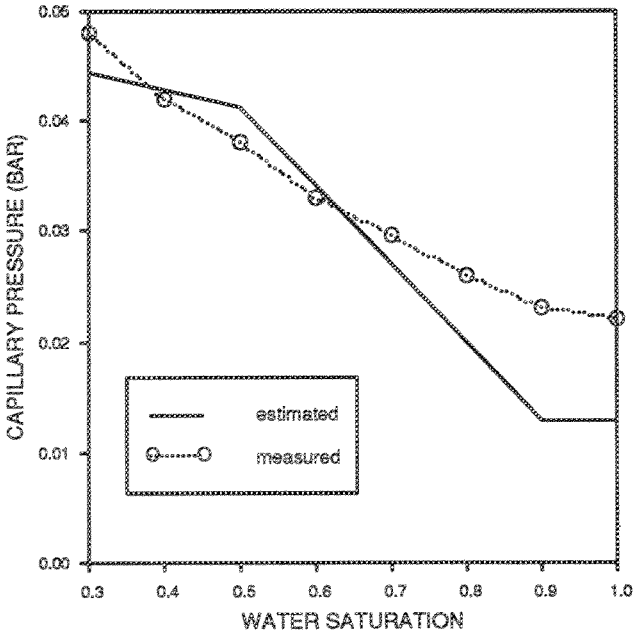

Figure 7 : Estimated Pc curve compared to the experimental curve.

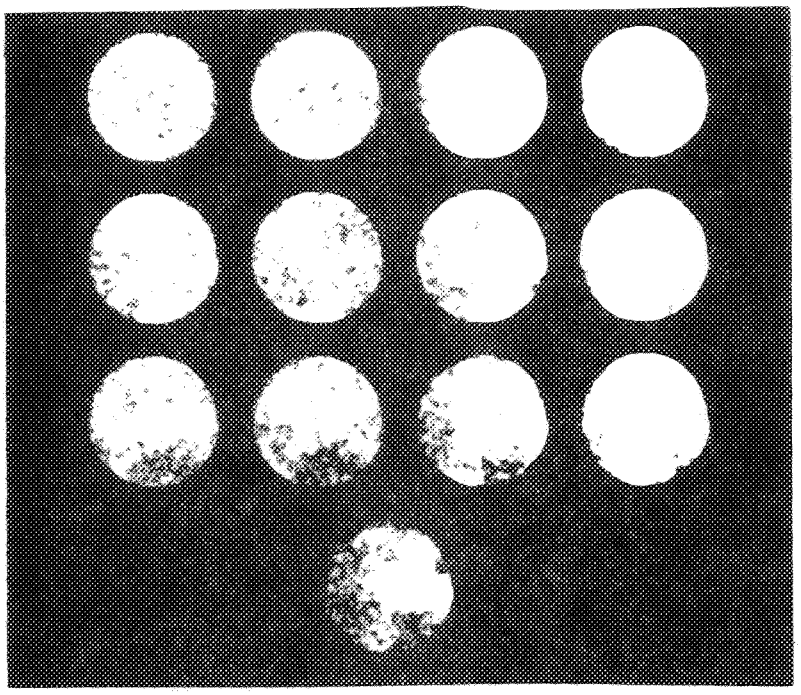

Figure 8 : 13 slices showing oil distribution.

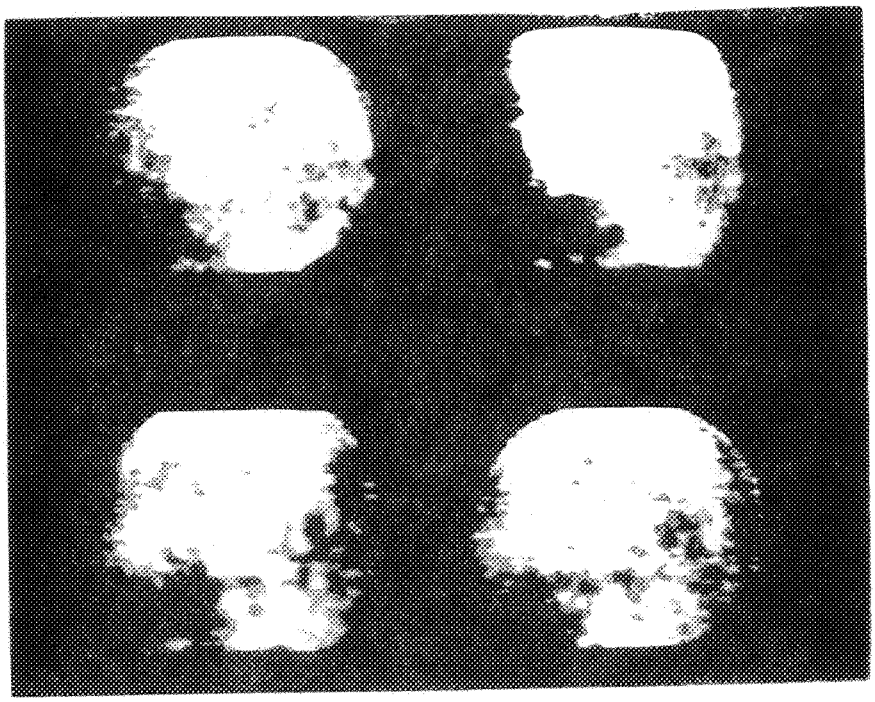

Figure 9 : 3-D reconstructions showing oil distribution.